

LIGHT SCATTERING IN THE LUNAR ORBITAL ENVIRONMENT BY NON-SPHERICAL DUST GRAINS. D. T. Richard^{1,2}, D. A. Glenar^{3,5}, T. J. Stubbs^{4,5}, S. S. Davis², and A. Colaprete^{2,5}, ¹San José State University Research Foundation, 210 N. Fourth St. Fourth Floor, San José, CA 95112, USA, ²Space Science and Astrobiology Division, NASA Ames Research Center, MS 245-3, Moffett Field, CA 94035-1000, USA, ³New Mexico State University, Las Cruces, New Mexico, USA, ⁴Goddard Earth Sciences and Technology Center, University of Maryland Baltimore County Baltimore, Maryland, USA, ⁵NASA Lunar Science Institute, NASA Research Park, Moffet Field, CA 94035.

Introduction: It is suspected that dust grains in the micron and submicron size range can be naturally transported by various electrostatic mechanisms above the surface of the Moon, to altitudes in excess of 100km [1], [2]. Evidence of a dust exosphere includes observations of "streamers" and "horizon glow" by Apollo Astronauts [3] as well as by the Surveyor landers [4] and Apollo coronal photography [5]. The scale-height of the observed horizon glow has been estimated to be 10km [1],[6].

The upper surface of the lunar regolith, from which this exospheric dust originates, is a layer of weakly cohesive particulate matter over the entirety of the lunar surface. Scanning electron photomicrographs of Apollo samples revealed the presence of a variety of grain morphology, from agglutinates with irregular and sharp edges to smoother glass droplets of volcanic origins [7] identify four prominent shapes for micrometer particles: spherical, angular blocks, glass shards and irregular.

Only recently was the ultra fine particle content of the regolith (<100 nm) measured [8]. The particles observed in the sub-micron range have compact ellipsoid shapes with small aspect ratios (i.e. close to spherical). Yet, based on the physical properties of small particulates and the extensive de-aggregation processes needed for their separation in the laboratory, it is unlikely for these grains to possess an individual dynamics; rather, they are expected to be transported either as aggregates or as parasites onto larger grains.

The shape of the particle scattering phase function conveys very important "1st order" information on the size of aerosol particles (both dust and volatiles). Likewise, the polarization state of this scattered light offers both size and shape information. The objective of our current project is therefore to compute the scattering properties of non-spherical lunar dust grain models using the Discrete Dipole Approximation (DDA)—which allows the determination of the scattering by targets of arbitrary morphology—for use in data analysis of optical diagnostics recorded in the lunar environment. We compare this model to the standard Mie theory for spherical particles.

Individual particle modeling: One objective of our project is the development of a "virtual lunar simu-

lant", a collection of numerical models of dust grains modeled in order that their computed scattering properties simulate those of the fine and ultra-fine fractions of the lunar regolith. In the same way that physical simulants are used in engineering model testing, our virtual simulant can be used in radiative transfer models. We demonstrate here the techniques we have developed and their usefulness with a limited preliminary set of target particles. Figure 1 shows the three grain morphologies we use here: i-an irregular particle to represent irregular, jagged micron and sub-micron dust grains; ii-a spherical particle with inclusions of nano-phasic Iron; iii-an aggregate of spherical monomers, to simulate the aggregation of ultra-fine grains.

The computations of the scattering signatures of the chosen target particles are accomplished with the publicly available code DDSCAT developed by Draine &

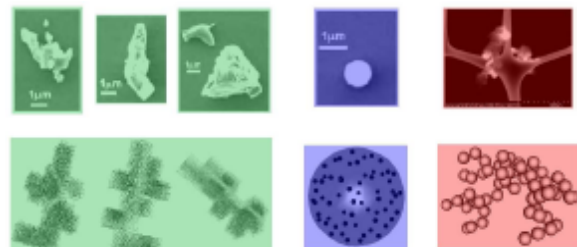


Figure 1: SEMs of lunar dust grains and corresponding numerical model.

Flatau (2004). DDSCAT is an implementation of the Discrete Dipole Approximation (DDA). The DDA approximates a continuum target by a finite array of polarizable points, allowing the computation of the scattering and absorption properties of targets of arbitrary geometry and heterogeneous composition.

Figure 2 shows the scattering and absorption efficiencies for the three types of targets from Fig. 1, compared to the standard Mie modeling of scattering by an homogeneous sphere. Significant differences are observed for sub-micron particles, down to a few tenths of a micron.

Application to orbital sensing of the lunar environment: The results of single particle scattering are then integrated into a light scattering code that simu-

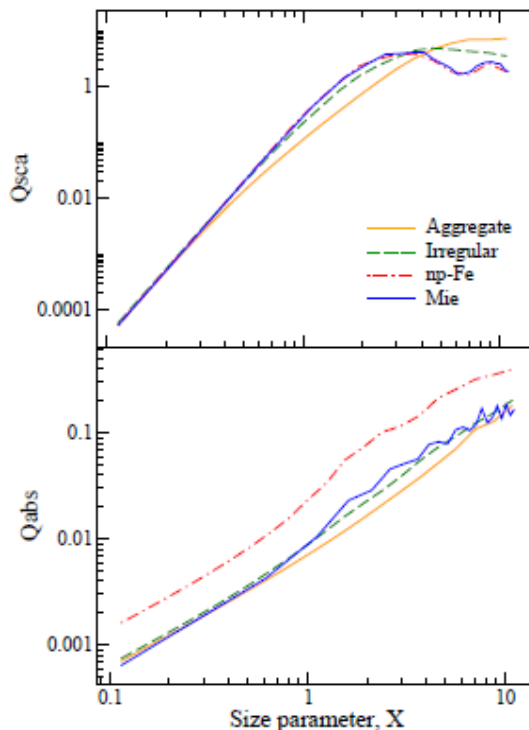


Figure 2: Scattering efficiency Q_{sca} (top) and absorption efficiency Q_{abs} (bottom) for aggregates (bold solid line), irregular particles (bolddashed line) and spherical grains containing np-Fe inclusions (bold dotted-dashed line), as computed through the DDA. Mie computation for an homogenous spherical particle is plotted for comparison (solid line).

lates the spectral intensity of the dust exosphere as would be observed by an orbiting spacecraft.

An Exosphere model is constructed from a modified Gamma Particle Size Distribution with $a_{peak} \sim 0.1$ microns. Small ($a \sim 0.1$ mm) particles dominate at $z \sim 10$ km. Figure 3 shows the spectrum of the lunar horizon glow that would be observed by the LADEE/UVS ultraviolet-visible spectrometer, as well as the observing limb geometry. Simulations were run for both (1) an equal-mass mixture of DDA-modeled complex particles (aggregate, irregular and np-Fe inclusions) and (2) Mie-modeled spherical homogeneous particles.

Computations for a set of diverse sample morphologies and compositions show that Mie theory can lead to large errors in predicted dust properties. In particular in this simulation, at large elongation angles, use of Mie theory to interpret measurements will underestimate the dust column abundance.

References: [1] Zook, H. A., & McCoy, J. E. (1991), *Geophys. Res. Lett.*, 18, 11, 2117. [2] Stubbs, T.J. et al, (2007), *Dust in Planetary Systems, (Workshop,*

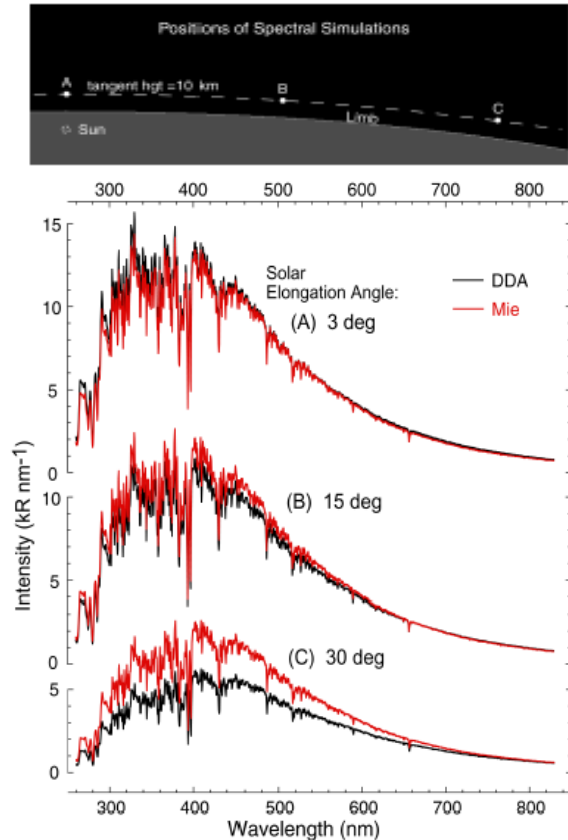


Figure 3: Simulations for a “UVS-like” spectrometer. Spacecraft at $z = 50$ km. Viewing sunrise horizon. Wavelength range 260–820 nm, Spectral resolution ~ 0.70 nm. On top is the limb viewing geometry showing the corresponding positions A, B and C.

September 26–30 2005, Kauai, HI), SP-643, pp. 239. [3] McCoy, J. E., & Criswell, D. R. (1974), *Proc. Lunar Sci. Conf. 5th*, 2991. [4] Rennilson, J. J., & Criswell, D. R. (1974), *The Moon*, 10/2, 121. [5] McCoy, J.E. (1976), *Proc. Lunar Sci. Conf. 7th*, 1087. [6] Murphy, D.L., and R.R. Vondrak (1993), *24th Lunar Planet. Sci. Conf.*, 1033–1034. [7] Park, J.S., Liu, Y., & Taylor, L.A. (2006), *37th Annual Lunar and Planetary Science Conference, March 13–17, 2006, League City, Texas*, abstract no.2193. [8] Greenberg, P. S., Chen, D., Smith, S. A. (2007), *NASA/TM-2007-214956*.